Acta Crystallographica Section D
Biological Crystallography
ISSN 0907-4449

The structure of a glycoside hydrolase family 81 endo-β-1,3-glucanase

Peng Zhou,[a] Zhongzhou Chen,[b] Qiaojuan Yan,[c] Shaoqing Yang,[a] Rolf Hilgenfeld[d] and Zhengqiang Jiang[a]*

[a]Department of Biotechnology, College of Food Science and Nutritional Engineering, China Agricultural University, Beijing 100083, People's Republic of China, [b]State Key Laboratory of Agrobiotechnology, China Agricultural University, Beijing 100193, People's Republic of China, [c]Bioresource Utilization Laboratory, College of Engineering, China Agricultural University, Beijing 100083, People's Republic of China, and [d]Institute of Biochemistry, University of Luebeck, Ratzeburger Allee 160, 23538 Luebeck, Germany

Correspondence e-mail: zhqjiang@cau.edu.cn

Received 21 April 2013
Accepted 29 June 2013

PDB References: *Rm*Lam81A, form I-free, 4k3a; form II-Se, 4k35

Endo-β-1,3-glucanases catalyze the hydrolysis of β-1,3-glycosidic linkages in glucans. They are also responsible for rather diverse physiological functions such as carbon utilization, cell-wall organization and pathogen defence. Glycoside hydrolase (GH) family 81 mainly consists of β-1,3-glucanases from fungi, higher plants and bacteria. A novel GH family 81 β-1,3-glucanase gene (*RmLam81A*) from *Rhizomucor miehei* was expressed in *Escherichia coli*. Purified *Rm*Lam81A was crystallized and the structure was determined in two crystal forms (form I-free and form II-Se) at 2.3 and 2.0 Å resolution, respectively. Here, the crystal structure of a member of GH family 81 is reported for the first time. The structure of *Rm*Lam81A is greatly different from all endo-β-1,3-glucanase structures available in the Protein Data Bank. The overall structure of the *Rm*Lam81A monomer consists of an N-terminal β-sandwich domain, a C-terminal $(\alpha/\alpha)_6$ domain and an additional domain between them. Glu553 and Glu557 are proposed to serve as the proton donor and basic catalyst, respectively, in a single-displacement mechanism. In addition, Tyr386, Tyr482 and Ser554 possibly contribute to both the position or the ionization state of the basic catalyst Glu557. The first crystal structure of a GH family 81 member will be helpful in the study of the GH family 81 proteins and endo-β-1,3-glucanases.

1. Introduction

The fungal cell wall with a rigid structure can protect the cell from osmotic pressure and other environmental stresses during the different stages of the life cycle. In almost all fungi, the central core of the cell wall is a branched β-1,3/1,6-glucan that is linked to chitin *via* a β-1,4 linkage (Latgé, 2007). Between 65 and 90% of the cell-wall glucan is found to be β-1,3-glucan (Bowman & Free, 2006). β-1,3-Glucan is also the main constituent of plant cell walls and a major structural and storage polysaccharide in marine macroalgae (Fibriansah *et al.*, 2007). Glycoside hydrolases (EC 3.2.1.*x*) form a widespread group of enzymes that hydrolyze the glycoside bond. Based on its mechanism of action, β-1,3-glucanase is classified as an endo-β-1,3-glucanase (laminarinase; EC 3.2.1.39) and an exo-β-1,3-glucanase (EC 3.2.1.58). The endo-β-1,3-glucanase cleaves within a glucan chain, releasing a mixture of oligosaccharides, while the exo-β-1,3-glucanase releases glucose residues from the nonreducing end (Martín-Cuadrado *et al.*, 2008).

According to the classification of carbohydrate-active enzymes (CAZy; http://www.cazy.org/; Cantarel *et al.*, 2009), endo-β-1,3-glucanases are grouped into six glycoside hydrolase (GH) families: 16, 17, 55, 64, 81 and 128 (Sakamoto *et al.*,

2011). Three-dimensional structures of members of GH families 16, 17, 55 and 64 have been solved, providing detailed structure–activity information (Wojtkowiak *et al.*, 2012). To date, no structural information has been reported on members of GH families 81 and 128.

So far, GH family 81 contains 175 members, which are widely distributed in fungi, higher plants and bacteria (http://www.cazy.org/GH81.html). All of the proteins share a common region of around 650 amino acids. Some members of this family have been characterized, such as *Aspergillus fumigatus* EngA (Fontaine *et al.*, 1997), *Saccharomyces cerevisiae* Eng2 (Martín-Cuadrado *et al.*, 2008), *Thermobifida fusca* Lam81 (McGrath & Wilson, 2006) and *Glycine max* β-glucan-binding protein (GBP) (Fliegmann *et al.*, 2005). All characterized GH family 81 proteins display endo-β-1,3-glucanase activity. Laminari-oligosaccharide degradation by GH family 81 endo-β-1,3-glucanase has revealed that the active site of the enzymes recognized at least five glucose units. ^{1}H NMR spectroscopic analysis has demonstrated that the enzymes utilize an inverting hydrolytic mechanism (Fliegmann *et al.*, 2005; McGrath & Wilson, 2006).

GH family 81 proteins show rather diverse physiological roles. GBP from the plant *G. max* is essential for a functional β-glucan receptor. It also shows β-1,3-glucanase activity (Umemoto *et al.*, 1997; Fliegmann *et al.*, 2005). GH family 81 endo-β-1,3-glucanases from bacteria such as *T. fusca* and *Bacillus halodurans* play a role in plant biomass degradation (van Bueren *et al.*, 2005; McGrath & Wilson, 2006). Eng1p from *S. cerevisiae* localizes to the daughter side of the septum and is involved in cell separation (Baladrón *et al.*, 2002). However, Eng1 from *S. pombe* localizes in a symmetrical fashion in a ring surrounding the primary septum during cell separation to hydrolyze the cell-wall components of the septum (Martín-Cuadrado *et al.*, 2003). *S. pombe* Eng2 acts together with a GH family 71 α-1,3-glucanase Agn2 in the last step in the sexual cycle for endolysis of the ascus wall (del Dedo *et al.*, 2009).

Rhizomucor miehei CAU432 is a strain of thermophilic fungus thriving at an optimum temperature at 323 K (Katrolia *et al.*, 2012). In the present study, cDNA cloning, heterologous expression, crystallization and two crystal structures of a recombinant endo-β-1,3-glucanase (*Rm*Lam81A) from *R. miehei* CAU432 are described. Like other members of GH family 81 proteins, *Rm*Lam81A exhibited β-1,3-glucanase activity and was active towards linear β-1,3-glucans (laminarin) with an endohydrolytic mode of action. The crystal structure of the enzyme is reported in two crystal forms, thereby providing the first three-dimensional structural view of a GH family 81 member.

2. Materials and methods

2.1. Cloning and expression

Recombinant DNA techniques as described by Sambrook & Russell (2001) were employed to perform DNA manipulations. The procedure described by Katrolia *et al.* (2012) was used with modifications to clone the endo-β-1,3-glucanase gene from *R. miehei* CAU432. Degenerate primers DP1 and DP2 (Supplementary Table S1[1]) were designed on the basis of the conserved sequences (YNDHHYH and DGRDQE) of fungal GH family 81 β-1,3-glucanases. The full-length cDNA sequence of the β-1,3-glucanase was obtained by 5′ and 3′ RACE (rapid amplification of cDNA end) using a SMART RACE cDNA Amplification Kit (Clontech). The β-1,3-glucanase cDNA sequence (designated as *RmLam81A*) from *R. miehei* CAU432 was deposited in the GenBank nucleotide sequence database with accession No. KC847083.

To express *RmLam81A*, the coding region of the gene without the signal peptide sequence was amplified by PCR from the cDNA of *R. miehei* CAU432 with primers *Rm*Lam81F and *Rm*Lam81R. *Bam*HI and *Xho*I sites (underlined) were added to the forward and reverse primers, respectively (Supplementary Table S1). The PCR product was cloned into the *Bam*HI/*Xho*I site of pET28a (+) vector (Novagen) and transformed into *Escherichia coli* BL21 for protein expression.

2.2. Purification

The *E. coli* BL21 transformant was grown in LB (Luria–Bertani) medium containing kanamycin (50 μg ml^{-1}) and incubated on a rotary shaker (200 rev min^{-1}, 310 K) until the optical density OD_{600} reached about 0.6–0.8. IPTG (isopropyl β-D-1-thiogalactopyranoside) was added to a final concentration of 1 m*M* to induce expression and the culture was grown at 303 K for a further 16 h. 1 l of *E. coli* culture was harvested by centrifugation, suspended in column buffer *A* (20 m*M* Tris–HCl pH 8.0, 500 m*M* NaCl, 20 m*M* imidazole) and disrupted by sonication. The lysate was clarified by centrifugation at 10 000*g* for 10 min at 277 K and the clear supernatant was applied onto an Ni–IDA column (1 × 5 cm; GE Life Sciences) pre-equilibrated with buffer *A*. The column was washed with buffer *A* followed by buffer *B* (20 m*M* Tris–HCl pH 8.0, 500 m*M* NaCl, 50 m*M* imidazole). The recombinant protein was eluted with buffer *C* (20 m*M* Tris–HCl pH 8.0, 500 m*M* NaCl, 200 m*M* imidazole). The purified β-1,3-glucanase (*Rm*Lam81A) was ultrafiltered, concentrated and buffer-exchanged in 100 m*M* Tris–HCl pH 8.0 using a 10 kDa molecular-weight cutoff ultrafiltration membrane. To remove the His tag, *Rm*Lam81A (1 mg ml^{-1}) was incubated with *B. subtilis* proteases (0.01 mg ml^{-1}) in 100 m*M* Tris–HCl pH 8.0 at 293 K overnight. The protein was further purified by gel filtration on a Sephacryl S-100 HR column in buffer *D* (20 m*M* Tris–HCl pH 8.0, 100 m*M* NaCl) and concentrated. Selenomethionine-derivatized *Rm*Lam81A was expressed using a metabolic inhibition protocol and M9 medium supplemented with 50 mg ml^{-1} L-selenomethionine (Se) and purified using the same protocol as described above.

[1] Supplementary material has been deposited in the IUCr electronic archive (Reference: DZ5286). Services for accessing this material are described at the back of the journal.

Table 1
X-ray data-collection and refinement statistics.

Values in parentheses are for the outer shell.

	Form I-free	Form II-Se
Data-collection statistics		
Radiation source	KEK-NE3A	SSRF-BL17U
Wavelength (Å)	0.9794	0.9792
Space group	$P12_11$	$P2_12_12_1$
Unit-cell parameters (Å, °)	a = 84.85, b = 91.63, c = 92.66, β = 98.71	a = 94.95, b = 118.66, c = 139.15
Resolution range (Å)	50.0–2.30 (2.34–2.30)	50.0–2.00 (2.03–2.00)
Total No. of reflections	303854	1317400
Unique reflections	61059	106346
Multiplicity	5.0 (4.3)	12.4 (9.5)
Completeness (%)	95.3 (83.5)	99.9 (98.3)
Mean $I/\sigma(I)$	23.4 (5.16)	42.8 (9.75)
$R_{\rm merge}$† (%)	9.7 (37.2)	9.5 (31.3)
B factor from Wilson plot (Å^2)	22.2	18.1
Refinement and model statistics		
Resolution (Å)	50.0–2.30 (2.34–2.30)	50.0–2.00 (2.03–2.00)
No. of reflections	59792	106200
$R_{\rm work}$‡ (%)	14.8 (18.1)	14.4 (17.1)
$R_{\rm free}$‡ (%)	19.7 (22.4)	17.6 (23.3)
No. of residues	1440	1433
No. of water molecules	699	1363
R.m.s.d., bond lengths (Å)	0.008	0.008
R.m.s.d., angles (°)	1.232	1.124
Mean B factor (Å^2)		
Main chain/side chain	12.9/14.4	8.4/12.3
Ligands/ions	30.9	19.4
Solvent	14.3	17.6
MolProbity statistics		
Ramachandran		
Most favoured (%)	97.13	97.24
Allowed (%)	2.73	2.62
Outliers (%)	0.14	0.14
Rotamer outliers (%)	1.88	0.97
Clashscore (%)	8.56	5.15
PDB code	4k3a	4k35

† $R_{\rm merge} = \sum_{hkl}\sum_i |I_i(hkl) - \langle I(hkl)\rangle| / \sum_{hkl}\sum_i I_i(hkl)$, where $I_i(hkl)$ is the intensity of observation i of reflection hkl and $\langle I(hkl)\rangle$ is the weighted average intensity for all observations i of reflection hkl. ‡ $R_{\rm work} = \sum_{hkl} ||F_{\rm obs}| - |F_{\rm calc}|| / \sum_{hkl} |F_{\rm obs}|$ for reflections in the working set, where $F_{\rm obs}$ and $F_{\rm calc}$ are the observed and calculated structure factors, respectively. $R_{\rm free}$ is calculated analogously for a test set of reflections that were randomly selected and excluded from the refinement.

2.3. Crystallization

Initial crystallization screening was performed manually using the Crystal Screen and Crystal Screen 2 reagent kits (Hampton Research) by vapour diffusion in sitting drops at 293 K in 48-well plates. Each drop consisted of 1 µl 20 mg ml^{-1} protein solution and 1 µl crystallization cocktail and was equilibrated against 100 µl reservoir solution.

Condition No. 17 of Crystal Screen [200 m*M* Li_2SO_4, 30%(*w*/*v*) PEG 4000, 100 m*M* Tris–HCl pH 8.5] was found to give clustered needle-shaped crystals in one week. The condition was further optimized by varying the precipitant, salt, buffer, pH and additives. Further crystallization trials yielded a cluster of plate-like crystals (form I-free) with optimal dimensions of 0.5 × 0.2 × 0.02 mm that grew in 160 m*M* Li_2SO_4, 24%(*w*/*v*) PEG 4000, 80 m*M* Tris–HCl pH 8.5, 6%(*v*/*v*) MPD (2-methyl-2,4-pentanediol) (Supplementary Fig. S1). Three plate-like crystals were directly flash-cooled in liquid nitrogen for data collection. One crystal diffracted to a resolution of 2.3 Å. The crystals took more than one month to grow and could not be reproduced. The other form of crystals (form II-Se) appeared using the condition 24%(*w*/*v*) PEG 4000, 80 m*M* Tris–HCl pH 8.5, 6%(*v*/*v*) MPD. The crystals appeared in 2–4 weeks with optimal dimensions of 0.4 × 0.2 × 0.2 mm (Supplementary Fig. S1). A single crystal of the Se-derivatized β-1,3-glucanase (form II-Se) picked up from a droplet in a 0.2 mm diameter mohair loop was transferred into cryoprotectant solution [24%(*w*/*v*) PEG 4000, 80 m*M* Tris–HCl pH 8.5, 30%(*v*/*v*) MPD] for 5 min and then placed directly into a liquid-nitrogen cryostream.

An X-ray diffraction data set was collected from a form I-free crystal using synchrotron radiation on beamline NE3A of the Photon Factory, High Energy Accelerator Research Organization (KEK), Tsukuba, Japan. Single-wavelength anomalous dispersion (SAD) data for the form II–Se crystals were collected on beamline BL-17U at the Shanghai Synchrotron Research Facility (SSRF), People's Republic of China. All diffraction data were indexed, integrated and scaled using the program *HKL*-2000 (Otwinowski & Minor, 1997).

The *Rm*Lam81A form I-free crystal had a monoclinic lattice (space group $P12_11$), with unit-cell parameters a = 84.85, b = 91.63, c = 92.66 Å. There were two molecules per asymmetric unit, with a corresponding Matthews coefficient ($V_{\rm M}$) of 2.23 Å^3 Da^{-1} and a solvent content of 44.9%. As no homologous structure of any member of GH family 81 had previously been determined, experimental phasing was necessary. To this end, Se-derivatized *Rm*Lam81A was prepared. The form II-Se crystal diffracted to 2.0 Å resolution and belonged to the orthorhombic space group $P2_12_12_1$, with unit-cell parameters a = 94.54, b = 118.66, c = 139.15 Å.

2.4. Structure determination and refinement

The *Rm*Lam81A structure was determined to 2.0 Å resolution by anomalous signal (Se-SAD) phasing techniques using the form II-Se crystal. For phasing experiments, *phenix.hyss* (Adams *et al.*, 2010) was used for determining the selenium substructures, *phenix.phaser* (McCoy *et al.*, 2007) was used for phasing, *phenix.resolve* (Terwilliger & Berendzen, 1999) was used for density modification and *phenix.autobuild* was used for automatic model building (Adams *et al.*, 2010). The experimentally phased electron-density map was of high quality, enabling 98% of the amino-acid sequence to be automatically traced using *phenix.autobuild*. The structure was completed with alternating rounds of manual model building with *Coot* (Emsley & Cowtan, 2004) and refinement with *phenix.refine* (Adams *et al.*, 2010). The *Rm*Lam81A form II-Se crystals contained two protein molecules, one MPD molecule and four Tris molecules in the asymmetric unit (Supplementary Fig. S2). The polypeptide chain of molecule *A* is visible from residues 6 to 724, with the N-terminal histidine tag, the first five residues and the C-terminal 47 residues not being visible in electron density. In molecule *B* a further seven disordered residues (Thr96–Asp103) could not be modelled because of poor electron density. The structure quality was

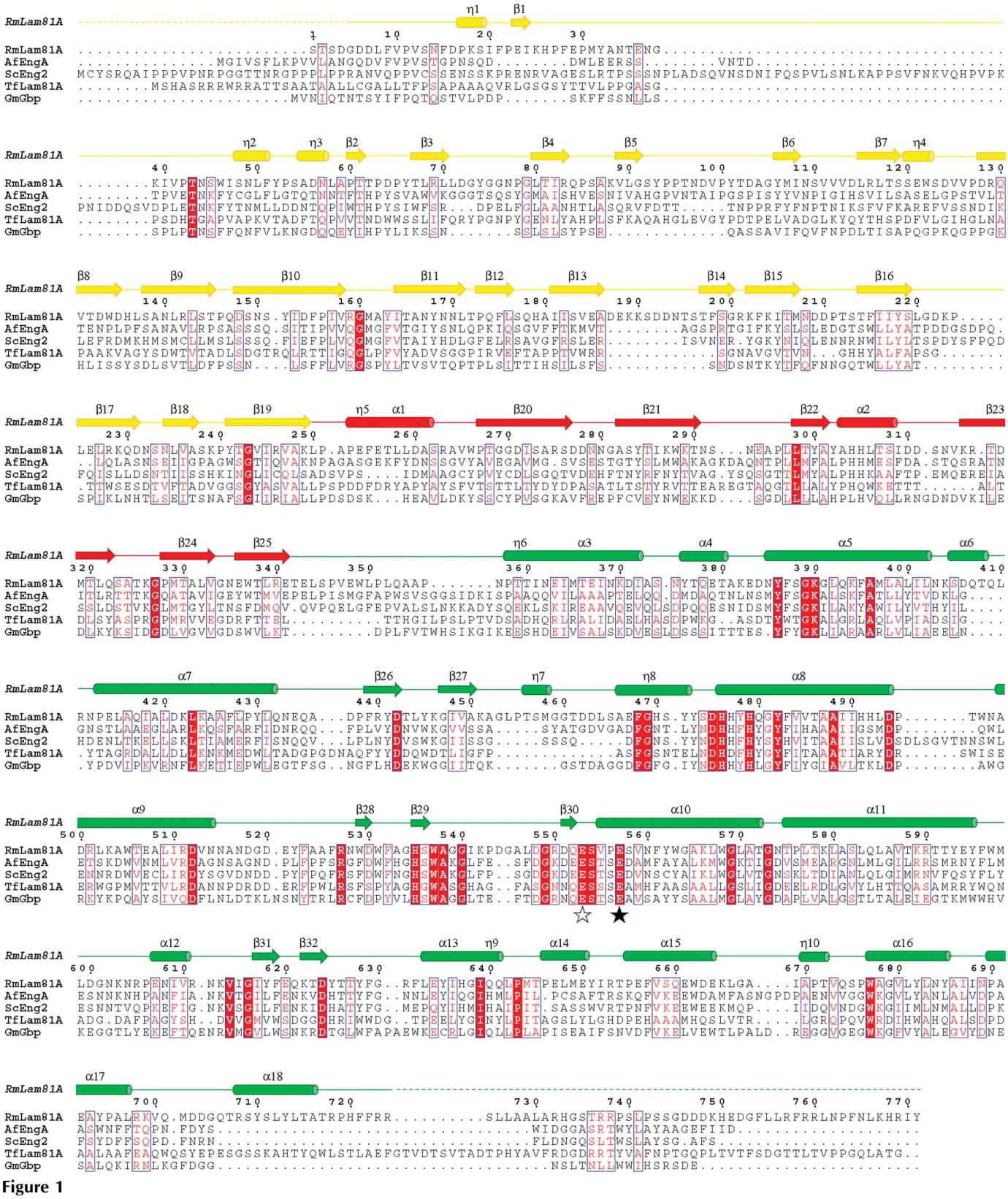

Figure 1
Structural sequence alignments of GH family 81 proteins. Residues forming the secondary structures are highlighted above the sequences of *Rm*Lam81A. Domain A, domain B and domain C are shown in yellow, red and green, respectively. The 3_{10}-helices are indicated by the character η. The identical residues are shown in white with a red background and conservative changes are shown in red with a white background. The catalytic residues are marked by empty (proton donor) and filled (basic catalyst) stars. The sequences of *R. miehei* GH family 81 β-1,3-glucanase (*Rm*Lam81A), *A. fumigatus* EngA (*Af*EngA; AAF13033), *S. cerevisiae* Eng2 (*Sc*Eng2; AAB82378), *T. fusca* YX Lam81A (*Tf*Lam81A, AAZ56163) and *G. max* Gbp (*Gm*Gbp; BAA11407) were aligned by *ClustalW*2 (Larkin *et al.*, 2007) and the figure was produced with *ESPript* (Gouet *et al.*, 2003) with manual modifications.

assessed by *MolProbity* (Chen *et al.*, 2010). The final model has a crystallographic R_{work} of 14.4% and an R_{free} of 17.6%. The average atomic *B* factor for the molecules is 9.7 Å^2.

For the form I-free structure, molecular replacement was used with the form II-Se crystal structure. *phenix.automr* and *phenix.autobuild* were utilized for molecular replacement and model rebuilding (Adams *et al.*, 2010). The structure was determined at 2.3 Å resolution. The *Rm*Lam81A form I-free crystals belonged to space group $P12_11$ and contained two protein molecules and two sulfate ions in the asymmetric unit (Supplementary Fig. S2). The final model has a crystallographic R_{work} of 14.8% and an R_{free} of 19.7%. The average atomic *B* factor for the molecule is 13.9 Å^2. The structure of *Rm*Lam81A was compared with all available protein structures using the *DALI* server (Holm & Rosenström, 2010). Structural superpositions were calculated using *LSQMAN* (Kleywegt, 1999). The solvent-accessible surface area was calculated using *AREAIMOL* in the *CCP*4 program suite, with a probe radius of 1.4 Å (Winn *et al.*, 2011). Analysis of the protein–ligand interactions was performed using the *LIGPLOT* program (Wallace *et al.*, 1995). Molecular and electron-density illustrations were prepared in *PyMOL* (v.1.3; Schrödinger LLC). The data-collection and refinement statistics of the final refined molecule geometry are listed in Table 1.

2.5. PDB accession code

The atomic coordinates and structure factors for the crystal structures of *Rm*Lam81A and its Se derivative have been deposited in the Protein Data Bank (PDB) under accession codes 4k3a and 4k35, respectively (http://www.pdb.org).

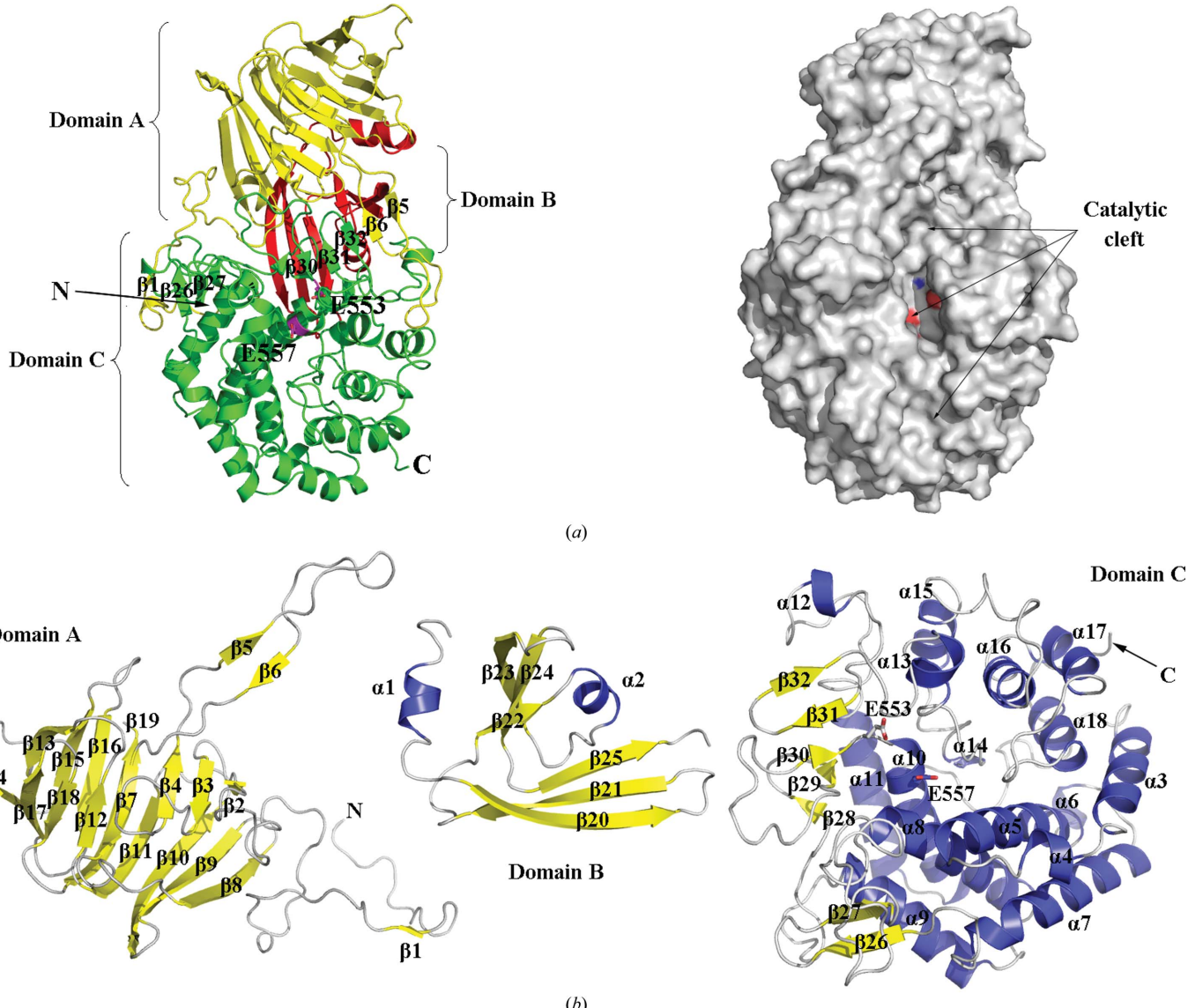

Figure 2
Structure of *R. miehei* GH family 81 β-1,3-glucanase (*Rm*Lam81A). (*a*) Ribbon representation and protein surface of *Rm*Lam81A. Domain A is coloured yellow, domain B red and domain C green. (*b*) Three-dimensional structure of *Rm*Lam81A domain A, domain B and domain C. The α-helical segments and β-strands are shown in blue and yellow, respectively. Catalytic residues (Glu553 and Glu557) are shown in stick representation. All figures were produced using *PyMOL* v.1.3 (http://www.pymol.org; Schrödinger LLC).

3. Results and discussion

3.1. Sequence analysis

Based on the conserved amino-acid sequences of fungal β-1,3-glucanase genes of GH family 81, a 341 bp fragment was amplified with degenerate primers LamDF and LamDR using genomic DNA from *R. miehei* CAU432 as the template. The 5′ and 3′ flanking regions of the fragment which were approximately 1663 and 846 bp, respectively, were then assembled with the core fragment to generate a 2489 bp cDNA sequence containing a putative full-length open reading frame (ORF) of 2391 bp (Supplementary Fig. S3). The translated protein contains 796 amino-acid residues. The nucleotide and deduced amino-acid sequences of the full-length cDNA and flanking region of the β-1,3-glucanase gene (*RmLam81A*) are shown in Fig. 1. Comparison of the cDNA with the genomic sequence indicated the existence of six introns in the coding region.

The N-terminal region (1–25) is predicted to be a signal peptide using the *SignalP*3.0 software (Bendtsen *et al.*, 2004). The mature protein contains 771 amino-acid residues with a predicted molecular mass of 87 kDa and a theoretical pI of 5.3. Like other fungal GH family 81 β-1,3-glucanases, *Rm*Lam81A contains a signal peptide suggesting that it is an extracellular protein.

According to the homology search by *PSI-BLAST* (Altschul *et al.*, 1997), the deduced amino-acid sequence of *Rm*Lam81A shows 60% identity (68% coverage) to a hypothetical protein from the zygomycota *Rhizopus delemar* (accession No. EIE78560). However, *Rm*Lam81A shows a relatively low degree (approximately 30%) of similarity to other fungal β-1,3-glucanases such as *A. fumigatus* EngA (*Af*EngA; 30% identity and 92% coverage; AAF13033; Fontaine *et al.*, 1997) and *S. cerevisiae* Eng2 (*Sc*Eng2; 27% identity and 92% coverage; AAB82378; Martín-Cuadrado *et al.*, 2008). The overall identity between *Rm*Lam81A and bacterial or plant proteins is also very low. The identity between *Rm*Lam81A and *T. fusca* Lam81 (*Tf*Lam81A; a bacterial protein; AAZ56163; McGrath & Wilson, 2006) and *G. max* β-glucan-elicitor receptor (*Gm*Gbp; a plant protein; BAA11407; Umemoto *et al.*, 1997) is only 20% (90% coverage) and 24% (88% coverage), respectively (Fig. 1).

3.2. Overall structures

The overall structure of *Rm*Lam81A is presented in Fig. 2. The *Rm*Lam81A monomer has approximate dimensions of 56.3 × 63.7 × 94.0 Å. The accessible surface area of the monomer to solvent is about 24 600 Å^2. The root-mean-square deviations (r.m.s.d.s) between two chains are 0.42 Å for *Rm*Lam81A form I-free crystal and 0.38 Å for *Rm*Lam81A form II-Se crystal over 710 and 709 matching C$^\alpha$ positions, respectively. Moreover, a comparison of the two chain structures of form I-free and form II-Se gives r.m.s.d.s ranging from 0.56 to 0.73 Å over 704–709 C$^\alpha$ atoms. The r.m.s.d. values indicate that the protein molecules between the two crystal forms are divergent. However, both crystal forms maintain the same secondary-structure elements and topologies. The highest atomic deviations are observed in the loop regions (Supplementary Fig. S4), especially for loops β3–β4 (Leu71–Pro78), β5–β6 (Ser92–Gly105) and β13–β14 (Glu187–Thr197). The conformational changes of loop β3–β4 (Leu71–Pro78) correlate with sulfate ion binding. The changes of loop β5–β6 (Ser92–Gly105) and loop β13–β14 (Glu187–Thr197) may be involved in crystal-packing interactions. The topology structure of *Rm*Lam81A is shown in Fig. 3. Each monomer of *Rm*Lam81A consists of 18 α-helices, 32 β-strands and ten 3_{10}-helices, comprising an N-terminal β-sandwich domain (domain A residues 1–250), a C-terminal $(\alpha/\alpha)_6$ domain (domain C residues 344–724) and an additional domain (domain B residues 251–343) between them (Fig. 2). There are two antiparallel β1–β26–β27, β30–β31–β32–β6–β5 cross-overs between domain A and domain C. Both domain A and domain C form the 'core' of *Rm*Lam81A which contributes to the active site and substrate-binding surface (Fig. 2).

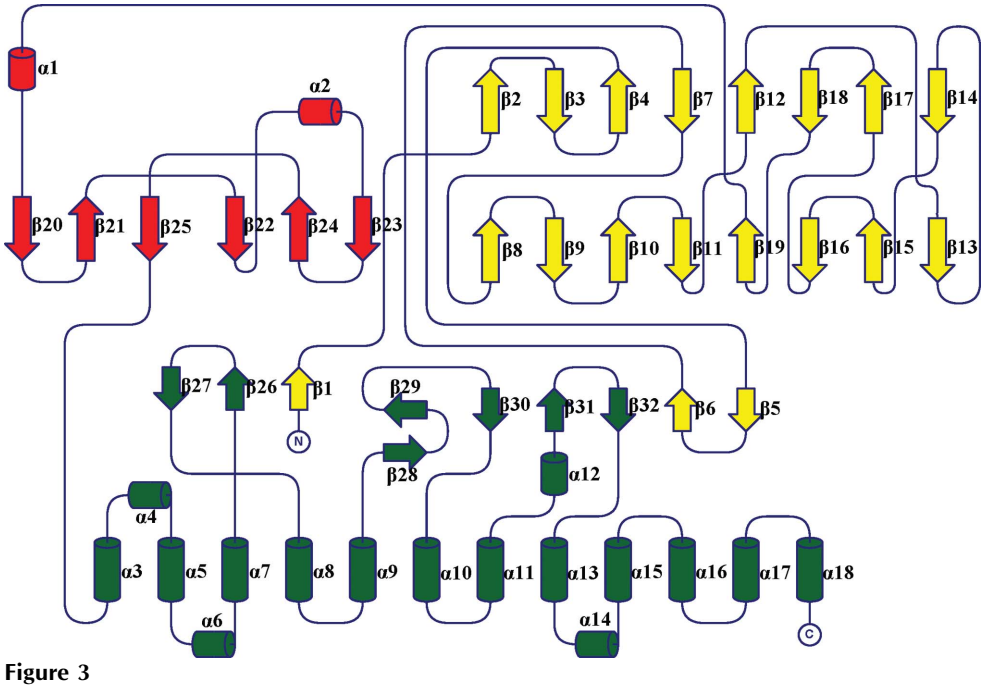

Figure 3
Topology of *Rm*Lam81A. β-Sheets are represented by arrows and α-helices are shown as cylinders surrounded by black boxes. The *Rm*Lam81A monomer is coloured according to the domains, with domain A depicted in yellow, domain B in red and domain C in green. This figure was drawn with *TopDraw* (Bond, 2003).

Domain A of *Rm*Lam81A consists of a core of two eight-

stranded antiparallel β-sheets with orders β2–β3–β4–β7–β12–β18–β17–β14 and β8–β9–β10–β11–β19–β16–β15–β13 packed on top of one another. According to the structural classification of proteins (SCOP; http://scop.berkeley.edu), this β-sandwich is grouped into the supersandwich superfamily, which contains 18 strands in two sheets (Murzin *et al.*, 1995). A structure-homologue search using the *DALI* server showed that domain A was best aligned with the β-sandwich of the GH family 57 4-α-glucanotransferase (TLGT) of *Thermococcus litoralis* (*Z*-score 11.0; PDB entry 1k1w; Imamura *et al.*, 2003) and the GH family 2 β-galactosidase (KL-β-Gal) from *Kluyveromyces lactis* (*Z*-score 10.6; PDB entry 3ob8; Pereira-Rodríguez *et al.*, 2012). TLGT is composed of two domains: an N-terminal domain (domain I), which contains a $(\beta/\alpha)_7$-barrel fold, and a C-terminal domain (domain II), which has a twisted β-sandwich fold (Imamura *et al.*, 2003). The KL-β-Gal subunit folds into five domains, only one (domain 3, TIM-barrel domain) of which has an assigned catalytic function (Pereira-Rodríguez *et al.*, 2012). Although the overall topology of the proteins is similar, the domains of *Rm*Lam81A, TLGT and KL-β-Gal differ markedly in overall atomic positions.

Domain C of *Rm*Lam81A is comprised of a core of $(\alpha/\alpha)_6$-barrel topology consisting of a double barrel of α-helices with the C-terminus of the outer helix leading into the N-terminus of an inner helix. According to the structural classification of proteins (SCOP), this $(\alpha/\alpha)_6$-barrel, which is common in glycosyl hydrolases, polysaccharide lyases and terpenoid cylases/protein prenyltransferases, is grouped into the six-hairpin enzyme superfamily (Murzin *et al.*, 1995). A structure-homologue search using the *DALI* server shows that domain C shares the highest structural similarity to the GH family 88 *Bacillus* sp. GL1 glycosaminoglycan (PDB entry 1vd5; *Z*-score 15.8; Itoh *et al.*, 2004) and the GH family 8 xylanase of *Pseudoalteromonas haloplanktis* (PDB entry 1h14; *Z*-score 15.2; Van Petegem *et al.*, 2003). Both these proteins show the same $(\alpha/\alpha)_6$-barrel fold found in the six-hairpin enzyme superfamily of the SCOP database.

Domain B of *Rm*Lam81A belongs to a short decoration linking domain A and domain C, which is located on the reverse side of *Rm*Lam81A. It contains two twisted antiparallel β-strands (β20–β21–β25 and β22–β24–β23) and two α-helices (Fig. 2*b*). On the surface of the *Rm*Lam81A structure there is a prominent cleft which is about 10 Å deep, 10 Å

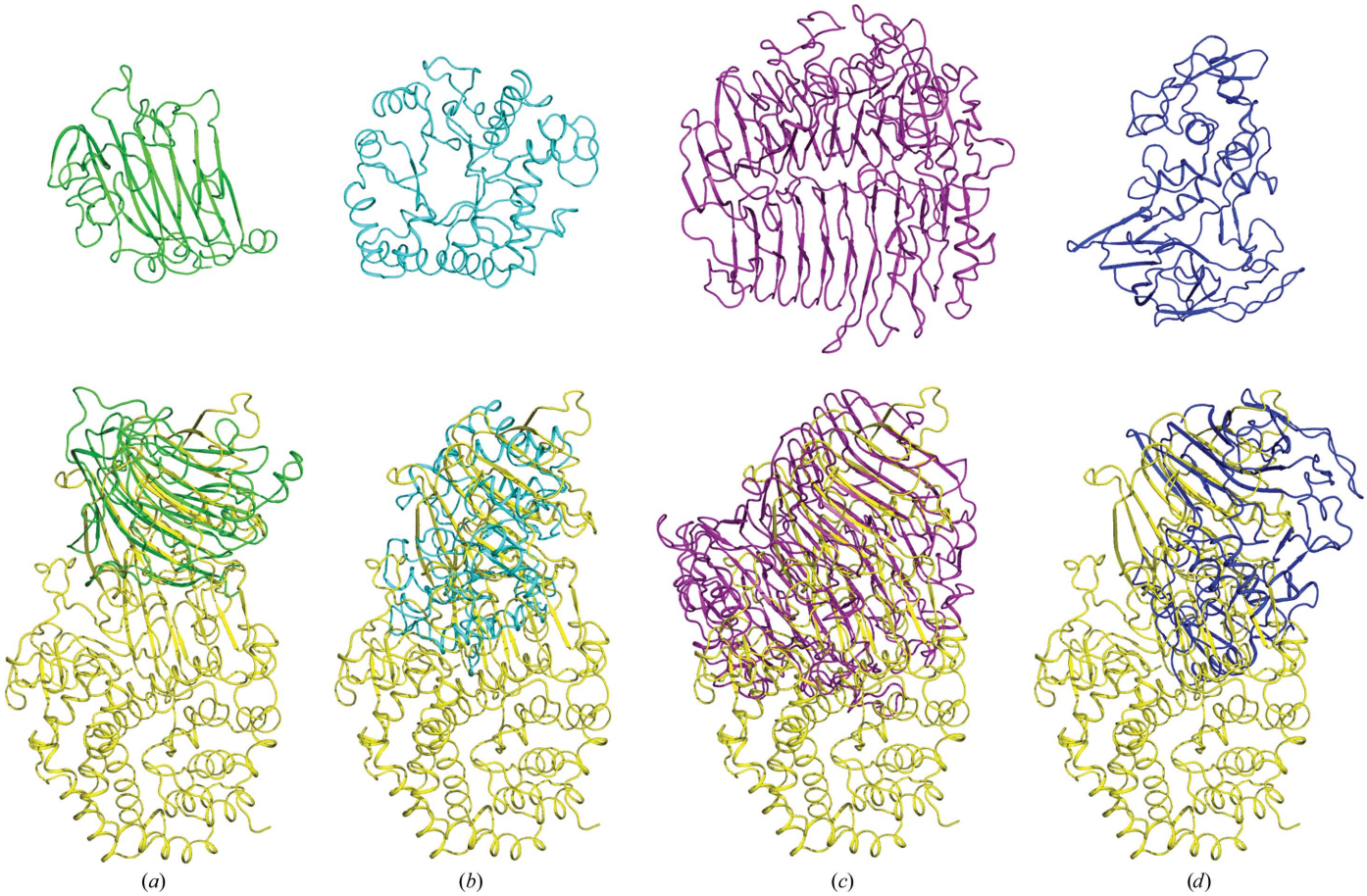

Figure 4
Cartoon representation of β-1,3-glucanases from other GH families: (*a*) GH family 16 (green; PDB entry 3azx; Jeng *et al.*, 2011), (*b*) GH family 17 (cyan; PDB entry 3ur7; Wojtkowiak *et al.*, 2012), (*c*) GH family 55 (purple; PDB entry 3eqn; Ishida *et al.*, 2009) and (*d*) GH family 64 β-1,3-glucanase (blue; PDB entry 3gd0; Wu *et al.*, 2009). The bottom panel shows the superposition of *Rm*Lam81A (yellow) and other glucanases. The structures were superimposed using the *SSM* algorithm in *Coot* (Emsley & Cowtan, 2004). All figures were produced using *PyMOL* v.1.3 (http://www.pymol.org; Schrödinger LLC).

wide and 70 Å long extending from domain C to domain A (Fig. 2*a*). The putative catalytic residues Glu553 and Glu557 sit in the middle of the cleft. The extended binding cleft is long enough to accommodate more than ten β-D-glucopyranosyl units. Long substrate-binding clefts with ends open at both sides have also been observed in many endoglucanases (Kitago *et al.*, 2007; Jeng *et al.*, 2011; Wojtkowiak *et al.*, 2013).

Although endo-β-1,3-glucanases from different GH families act on similar substrates, they have evolutionarily distinct folds (Fig. 4). GH family 16 endo-β-1,3-glucanases from bacteria have a classical sandwich-like β-jelly-roll fold composed of two antiparallel β-sheets packed against each other (Fibriansah *et al.*, 2007; Jeng *et al.*, 2011), whereas GH family 17 endo-β-1,3-glucanases from plants adopt an $(\alpha/\beta)_8$ TIM-barrel fold (Wojtkowiak *et al.*, 2012, 2013). GH family 55 endo-β-1,3-glucanases from fungi contain two domains with a right-handed parallel β-helix fold forming a ribcage-like overall architecture (Ishida *et al.*, 2009). GH family 64 endo-β-1,3-glucanases from bacteria consist of a barrel domain and a mixed (α/β) domain forming a two-domain crescent architecture (Wu *et al.*, 2009). The structure of *Rm*Lam81A was different from all endo-β-1,3-glucanase structures available in the PDB. A structural similarity search using the *DALI* server revealed that *Rm*Lam81A has no homology with the structures of β-1,3-glucanases from other GH families (a *DALI* *Z*-score of <2). In *Rm*Lam81A, domain A without catalytic function adopts a β-sandwich fold and reveals different protein folds as observed in the GH 16 family enzymes. In the CAZY enzymes, GH families 8, 15, 37, 48, 63, 65, 88, 105, 125 and 126 also display this $(\alpha/\alpha)_6$-barrel motif (Cantarel *et al.*, 2009). The catalytic centre of these enzymes is located on one side of the barrel, such as in the GH family 8 xylanase of *P. haloplanktis* (Van Petegem *et al.*, 2003) and GH family 15 *Trichoderma reesei* glucoamylase (PDB entry 2vn4; Bott *et al.*, 2008). GH families 8, 88, 105 and 125 consist of a single $(\alpha/\alpha)_6$-barrel domain (Van Petegem *et al.*, 2003; Itoh *et al.*, 2004; Zhang *et al.*, 2005; Gregg *et al.*, 2011). However, GH families 48 and 63 have a more complex structure. The GH family 48 CelF of *Clostridium cellulolyticum* has an $(\alpha/\alpha)_6$-barrel with long loops on the N-terminal side of the inner helices (a *DALI* *Z*-score of 9.8 compared with *Rm*Lam81A domain C), which form a tunnel, and an open cleft region covering one side of the barrel (PDB entry 1f9d; Parsiegla *et al.*, 1998). The GH family 63 α-glucosidase (Ygjk) of *E. coli* is composed of a super-β-sandwich N-domain (a *DALI* *Z*-score of 7.9 compared with *Rm*Lam81A domain A) and an $(\alpha/\alpha)_6$-barrel A domain (a *DALI* *Z*-score of 12.8 compared with the *Rm*Lam81A domain C; PDB entry 3d3i; Kurakata *et al.*, 2008). However, the overall structure of *Rm*Lam81A compared with Ygjk shows a *DALI* *Z*-score of 9.4.

In previous research, the biochemical activity of endo-β-1,3-glucanase from *A. fumigatus* (*Af*Engl1) has been described. Although the minimum substrate cleaved was laminaritetraose, laminaritetraose was degraded very poorly, suggesting that the natural substrate has at least five glucose residues (Fontaine *et al.*, 1997). Similar results were also observed in *Sp*Eng1, *Sp*Eng2, *Sc*Eng2 and *Gm*GBP (Fliegmann *et al.*, 2005; Martín-Cuadrado *et al.*, 2008). Besides, *Af*Engl1 was more efficient in catalyzing the hydrolysis of longer oligosaccharides. The K_m values of *Af*Engl1 were similar (around 0.3 mg ml^{-1}) for all reduced soluble substrates with different sizes such as reduced pentasaccharides, hexasaccharides, octasaccharides and oligosaccharides; the V_{max} values increased with the size of the substrate. The velocity of the catalytic reaction increased with the number of β-1,3-glycosidic bonds in the substrate, since the size of the soluble substrate did not modify the affinity of the enzyme (Fontaine *et al.*, 1997). This finding is possibly explained by the structural evidence of *Rm*Lam81A, which has a long cleft on the surface.

3.3. Tris, MPD and sulfate ion sites

There are two Tris binding sites found in the form II-Se crystal structure (Fig. 5*a* and Supplementary Fig. S5*a*). The first Tris is present in the vicinity of catalytic residues Glu553 (proton donor) and Glu557 (basic catalyst). This Tris molecule made a network of six hydrogen bonds with the three residues Asp475, His479 and Glu557 and three water molecules. In addition, it formed two hydrogen bonds to Glu553 mediated by water molecules. The second Tris molecule made a network of five hydrogen bonds to the two residues Asp98, Glu634 and two water molecules (Fig. 5*b* and Supplementary Fig. S5*b*). In the form II-Se crystal structure, a clear electron density corresponding to an MPD molecule was present between the protein molecules. The MPD molecule makes only one hydrogen bond to a water molecule (Fig. 5*c* and Supplementary Fig. S5*c*). There is a sulfate ion (SO_4^{2-}) binding site found in the form I-free crystal structure. The sulfate ion is coordinated to seven atoms: four backbone N atoms (Tyr74, Gly75, Gly76 and Asn77) which belong to a small loop $\beta3$–$\beta4$ (Leu71–Pro78), the N$^{\eta}$1 atom of Arg116 and two water molecules. Superposition of the form I-free and form II-Se crystal structures showed a high atomic deviation in the loop regions (Fig. 5*d* and Supplementary Fig. S5*d*). There was no electron density of Tris or MPD molecules found in the form I-free crystal structure.

Ligands serve to stabilize the protein, thereby reducing its propensity to unfold, aggregate or succumb to proteolysis, and have been used to increase the success rate of protein stability, crystallization and structure determination (Vedadi *et al.*, 2006). The Tris molecule as a competitive inhibitor has often been observed in the structures of some enzymes (Bott *et al.*, 2008; Tsai *et al.*, 2011). Structure analysis showed that the Tris molecule may work as an inhibitor and bind in the active centre (Fig. 5*a*). MPD was imported during the crystallization and cooling. A high concentration of MPD existed in the crystal and cryoprotectant solutions. It was not surprising that the form II-Se crystals grow in nearly the same conditions as the form I-free crystals, except for the presence of Li_2SO_4, as a sulfate ion was bound tightly to the *Rm*Lam81A structure.

3.4. The catalytic cleft and the active site

Amino-acid sequence alignments of GH family 81 members revealed that 37 residues were strictly conserved (Fig. 1).

Among them, Tyr386, Lys390, Phe468, Asp475, His479, Tyr482, Glu553, Ser554, Glu557, Pro643, Ile639 and Try677 were located in the substrate-binding cleft (Fig. 6*a*). Along the catalytic cleft there are a number of aromatic residues (Figs. 6*c* and 6*d*; Phe387, Phe468, Tyr628, Phe629 and Trp677) that are conserved (Fig. 1; Tyr628 and Phe629 can be replaced by other aromatic residues) in GH family 81 glucanases and may be involved in stacking interactions with the rings of the glucosyl residues of the substrate.

Usually, hydrolysis of glycoside bonds takes place *via* a general acid catalysis mechanism which requires two acidic residues. In inverting glycosidases, the two carboxyl groups serve as a proton donor and nucleophile (basic catalyst), respectively (Zechel & Withers, 1999; Wu *et al.*, 2009). The *Rm*Lam81A substrate-binding cleft only has three conserved acidic residues, including two Glu residues (Glu553 and Glu557) and one Asp residue (Asp475). According to a previously reported study, Asp526 in *Sc*Eng2 (at the same position as Asp475 in *Rm*Lam81A) is not critical in hydrolysis of the glycoside bonds (Martín-Cuadrado *et al.*, 2008). Thus, Glu553 and Glu557 might be catalytic residues. During the glycosylation reaction, carboxyl groups that serve as proton donors must initially be protonated, whereas carboxyl groups that function as base catalysts (nucleophiles) must be negatively charged (Zechel & Withers, 1999). The enzyme structures have evolved in part to modulate the physicochemical properties of those amino acids, giving them distinct pK_a values (Joshi *et al.*, 2001). In the *Rm*Lam81A structure, Glu553 did not form any hydrogen bonds to other amino acids and was located in a relatively hydrophobic environment, while

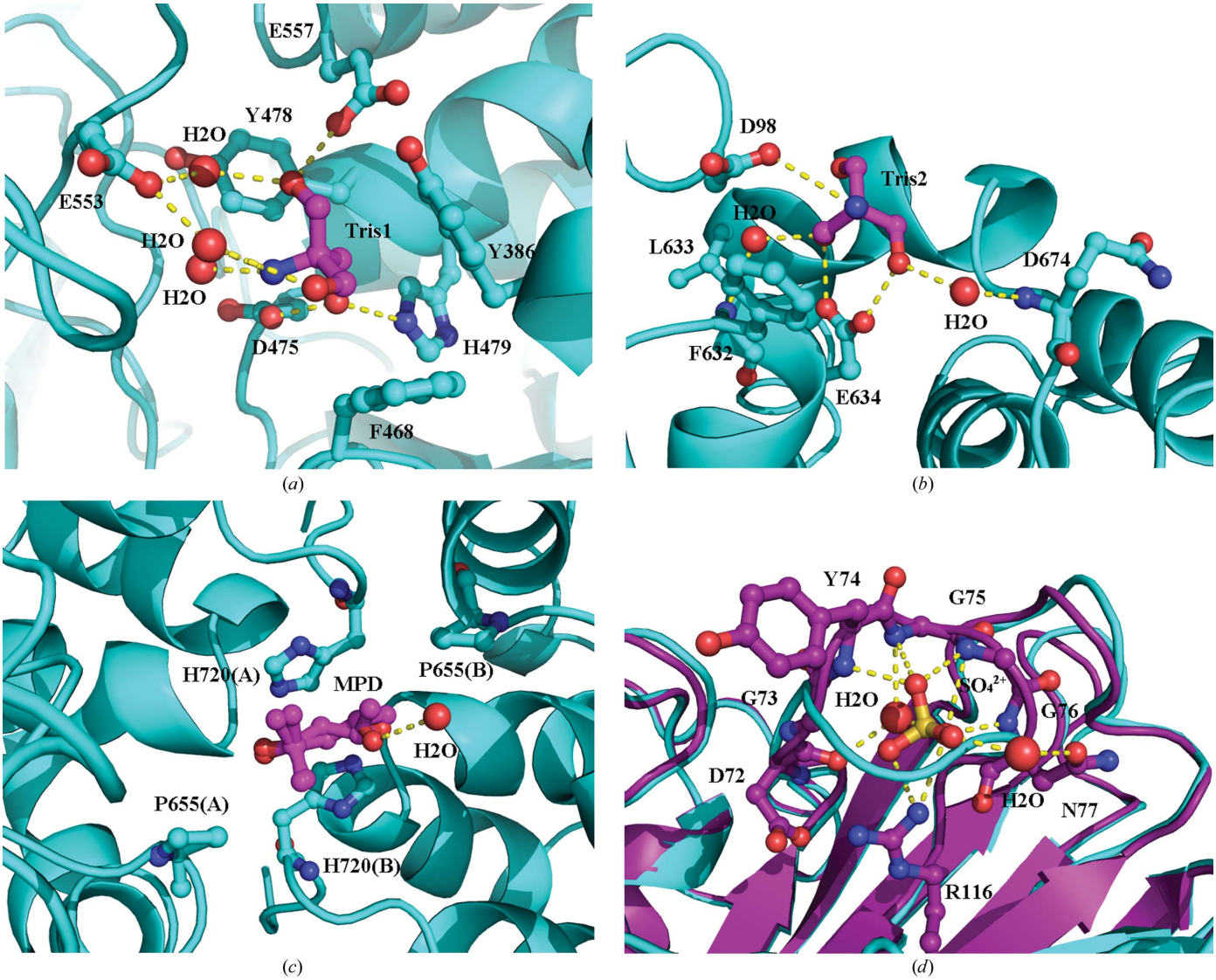

Figure 5
Stereoview of the interactions between the *Rm*Lam81A form II-Se protein with (*a*) the primary Tris molecule (Tris1), (*b*) the second Tris molecule (Tris2), (*c*) the MPD molecule and (*d*) the form I-free protein with sulfate ion. *Rm*Lam81A form I-free structure is coloured purple and the form II-Se structure is coloured blue. The side chains and backbone atoms of protein residues involved in ligand binding are shown in ball-and-stick representation. Water molecules are depicted as spheres and hydrogen-bond interactions are shown as dotted lines. All figures were produced using *PyMOL* v.1.3 (http://www.pymol.org; Schrödinger LLC).

Glu557 formed hydrogen bonds to Tyr386 and Tyr482, which are highly conserved in all GH family 81 members (Fig. 6*b*). The polar environment of Glu557 is supposed to maintain the ionization state. Therefore, Glu553 and Glu557 are likely to serve as a proton donor and a basic catalyst, respectively. In addition to the catalytic residues, Ser554 plays an important role in stabilizing the position of Glu557 by making a hydrogen bond to the backbone N atom, which is highly conserved in all GH family 81 members.

Furthermore, hydrolysis of the glycosidic bond can occur with one of two possible stereochemical outcomes: inversion or retention of anomeric configuration (Zechel & Withers, 1999). The two carboxyl groups in inverting glycosidases serve as a proton donor and a basic catalyst and are suitably placed, on average 10.5 Å apart, to allow the substrate and a water molecule to bind between them. By contrast, the carboxyl groups in retaining glycosidases are only 5.5 Å apart (Zechel & Withers, 1999). The distance between the two catalytic amino acids (Glu553 and Glu557; from C^{δ} to C^{δ}) in *Rm*Lam81A is 8.7 Å. Therefore, the hydrolytic catalysis of *Rm*Lam81A might be based on the inversion mechanism. This structural evidence agrees with the results from the ^{1}H NMR

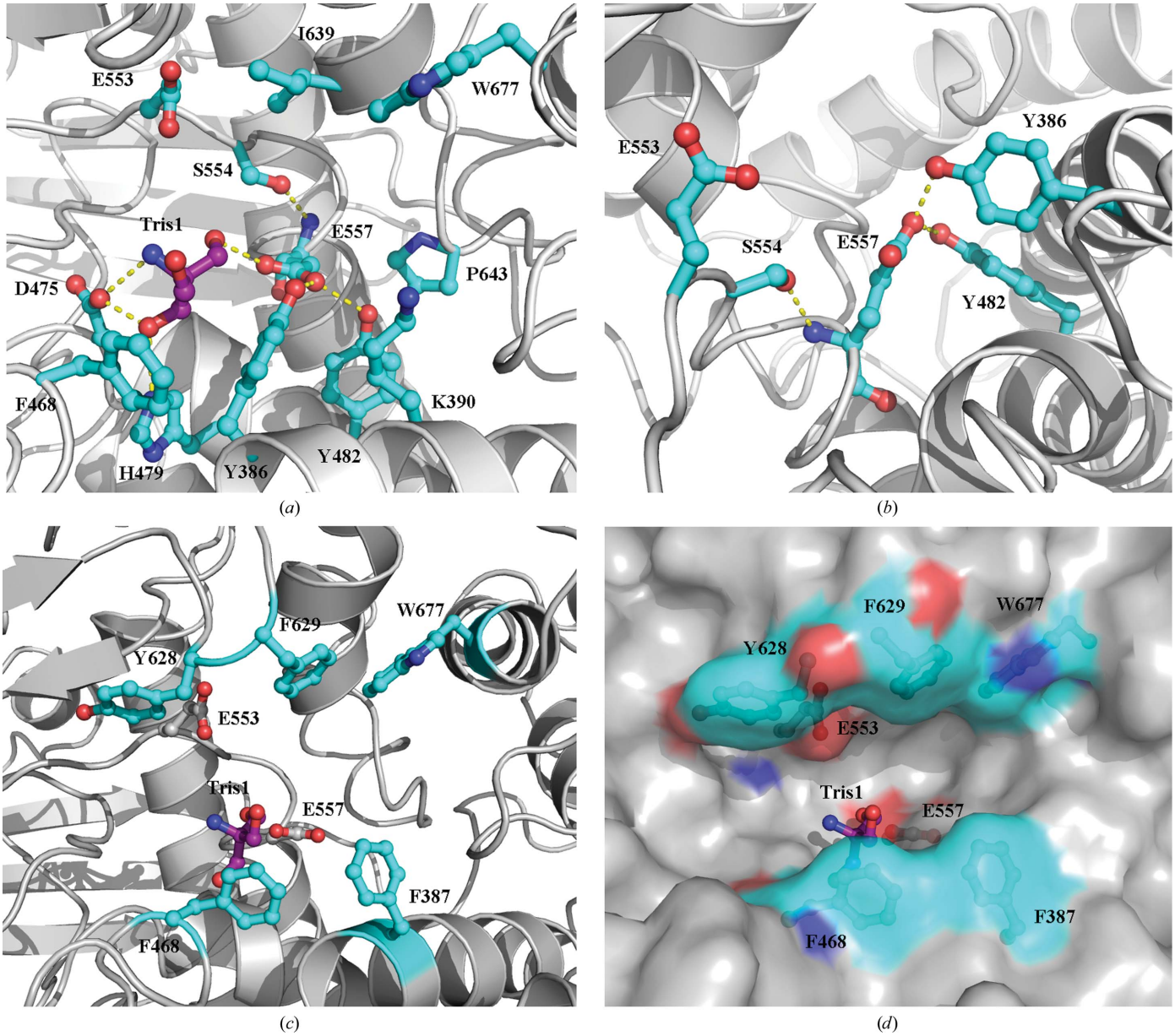

Figure 6
Representation of the active site and substrate-binding cleft. (*a*) Highly conserved residues in the active site. The *Rm*Lam81A structure (grey) complexed with Tris (purple), depicting the highly conserved residues in GH family 81: Tyr386, Lys390, Phe468, Asp475, His479, Tyr482, Glu553, Ser554, Glu557, Pro643, Ile639 and Trp677. (*b*) Close-up of the active site showing the catalytic site residues and the conserved hydrogen bonding between them. (*c*) A number of conserved aromatic residues, Phe387, Phe468, Tyr628, Phe629 and Trp677, along the catalytic cleft. (*d*) Surface representation of the *Rm*Man5B catalytic gorge, with the conserved aromatic residues shown in ball-and-stick mode. All figures were produced using *PyMOL* v.1.3 (http://www.pymol.org; Schrödinger LLC).

spectrum during the hydrolysis of laminarin by soybean GBP (Fliegmann *et al.*, 2005) and *T. fusca* Lam81A (McGrath & Wilson, 2006).

4. Conclusions

The crystal structure of the endo-β-1,3-glucanase as a member of GH family 81 from the thermophilic fungus *R. miehei* was determined in two different crystal forms (form I-free and form II-Se) to resolutions of 2.3 and 2.0 Å, respectively. The enzyme has three distinct domains: domain A (residues 1–250), domain B (residues 251–343) and domain C (residues 344–724). Domain A has a core of two eight-stranded antiparallel β-sheets. Domain C is comprised of an $(\alpha/\alpha)_6$-barrel. Domain A and domain C form the 'core' of the enzyme. Domain A compacts with domain C and forms a long binding cleft. The cleft is long enough to accommodate more than ten β-D-glucopyranosyl units. Domain B, which is conserved in all GH family 81 members, exists on the reverse side of *Rm*Lam81A and is likely to stabilize the whole structure. A Tris molecule is likely to act as an inhibitor and binds in the active site, thus stabilizing the structure. On the basis of previous studies, we can deduce that Glu553 and Glu557 might be a proton donor and a basic catalyst, respectively. In addition, Tyr386, Tyr482 and Ser554 contribute to both the position or ionization state of these critical residues. The distance between the two catalytic residues (Glu553 and Glu557) is 8.7 Å. The structural evidence agrees with the results that the hydrolytic catalysis might possibly be based on the inversion mechanism.

This work was supported in part by the National Natural Science Foundation of China (Project No. 31071508) and the German fellowship programme for S&T awardees. We are grateful to the staff of the SSRF and KEK for their assistance in X-ray data collection.

References

Adams, P. D. *et al.* (2010). *Acta Cryst.* D**66**, 213–221.
Altschul, S. F., Madden, T. L., Schaffer, A. A., Zhang, J., Zhang, Z., Miller, W. & Lipman, D. J. (1997). *Nucleic Acids Res.* **25**, 3389–3402.
Baladrón, V., Ufano, S., Dueñas, E., Martín-Cuadrado, A.-B., del Rey, F. & Vázquez de Aldana, C. R. (2002). *Eukaryot. Cell*, **1**, 774–786.
Bendtsen, J. D., Nielsen, H., von Heijne, G. & Brunak, S. (2004). *J. Mol. Biol.* **340**, 783–795.
Bond, C. S. (2003). *Bioinformatics*, **19**, 311–312.
Bott, R., Saldajeno, M., Cuevas, W., Ward, D., Scheffers, M., Aehle, W., Karkehabadi, S., Sandgren, M. & Hansson, H. (2008). *Biochemistry*, **47**, 5746–5754.
Bowman, S. M. & Free, S. J. (2006). *Bioessays*, **28**, 799–808.
Bueren, A. L. van, Morland, C., Gilbert, H. J. & Boraston, A. B. (2005). *J. Biol. Chem.* **280**, 530–537.
Cantarel, B. L., Coutinho, P. M., Rancurel, C., Bernard, T., Lombard, V. & Henrissat, B. (2009). *Nucleic Acids Res.* **37**, D233–D238.
Chen, V. B., Arendall, W. B., Headd, J. J., Keedy, D. A., Immormino, R. M., Kapral, G. J., Murray, L. W., Richardson, J. S. & Richardson, D. C. (2010). *Acta Cryst.* D**66**, 12–21.
Emsley, P. & Cowtan, K. (2004). *Acta Cryst.* D**60**, 2126–2132.
Encinar del Dedo, J., Dueñas, E., Arnáiz, Y., del Rey, F. & Vázquez de Aldana, C. R. (2009). *Eukaryot. Cell*, **8**, 1278–1286.
Fibriansah, G., Masuda, S., Koizumi, N., Nakamura, S. & Kumasaka, T. (2007). *Proteins*, **69**, 683–690.
Fliegmann, J., Montel, E., Djulić, A., Cottaz, S., Driguez, H. & Ebel, J. (2005). *FEBS Lett.* **579**, 6647–6652.
Fontaine, T., Hartland, R. P., Beauvais, A., Diaquin, M. & Latgé, J.-P. (1997). *Eur. J. Biochem.* **243**, 315–321.
Gouet, P., Robert, X. & Courcelle, E. (2003). *Nucleic Acids Res.* **31**, 3320–3323.
Gregg, K. J., Zandberg, W. F., Hehemann, J. H., Whitworth, G. E., Deng, L., Vocadlo, D. J. & Boraston, A. B. (2011). *J. Biol. Chem.* **286**, 15586–15596.
Holm, L. & Rosenström, P. (2010). *Nucleic Acids Res.* **38**, W545–W549.
Imamura, H., Fushinobu, S., Yamamoto, M., Kumasaka, T., Jeon, B.-S., Wakagi, T. & Matsuzawa, H. (2003). *J. Biol. Chem.* **278**, 19378–19386.
Ishida, T., Fushinobu, S., Kawai, R., Kitaoka, M., Igarashi, K. & Samejima, M. (2009). *J. Biol. Chem.* **284**, 10100–10109.
Itoh, T., Akao, S., Hashimoto, W., Mikami, B. & Murata, K. (2004). *J. Biol. Chem.* **279**, 31804–31812.
Jeng, W.-Y., Wang, N.-C., Lin, C.-T., Shyur, L.-F. & Wang, A. H.-J. (2011). *J. Biol. Chem.* **286**, 45030–45040.
Joshi, M. D., Sidhu, G., Nielsen, J. E., Brayer, G. D., Withers, S. G. & McIntosh, L. P. (2001). *Biochemistry*, **40**, 10115–10139.
Katrolia, P., Jia, H., Yan, Q., Song, S., Jiang, Z. & Xu, H. (2012). *Bioresour. Technol.* **110**, 578–586.
Kitago, Y., Karita, S., Watanabe, N., Kamiya, M., Aizawa, T., Sakka, K. & Tanaka, I. (2007). *J. Biol. Chem.* **282**, 35703–35711.
Kleywegt, G. J. (1999). *Acta Cryst.* D**55**, 1878–1884.
Kurakata, Y., Uechi, A., Yoshida, H., Kamitori, S., Sakano, Y., Nishikawa, A. & Tonozuka, T. (2008). *J. Mol. Biol.* **381**, 116–128.
Larkin, M. A., Blackshields, G., Brown, N. P., Chenna, R., McGettigan, P. A., McWilliam, H., Valentin, F., Wallace, I. M., Wilm, A., Lopez, R., Thompson, J. D., Gibson, T. J. & Higgins, D. G. (2007). *Bioinformatics*, **23**, 2947–2948.
Latgé, J.-P. (2007). *Mol. Microbiol.* **66**, 279–290.
Martín-Cuadrado, A.-B., Dueñas, E., Sipiczki, M., Vázquez de Aldana, C. R. & del Rey, F. (2003). *J. Cell Sci.* **116**, 1689–1698.
Martín-Cuadrado, A.-B., Fontaine, T., Esteban, P.-F., del Dedo, J. E., de Medina-Redondo, M., del Rey, F., Latgé, J.-P. & de Aldana, C. R. (2008). *Fungal Genet. Biol.* **45**, 542–553.
McCoy, A. J., Grosse-Kunstleve, R. W., Adams, P. D., Winn, M. D., Storoni, L. C. & Read, R. J. (2007). *J. Appl. Cryst.* **40**, 658–674.
McGrath, C. E. & Wilson, D. B. (2006). *Biochemistry*, **45**, 14094–14100.
Murzin, A. G., Brenner, S. E., Hubbard, T. & Chothia, C. (1995). *J. Mol. Biol.* **247**, 536–540.
Otwinowski, Z. & Minor, W. (1997). *Methods Enzymol.* **276**, 307–326.
Parsiegla, G., Juy, M., Reverbel-Leroy, C., Tardif, C., Belaïch, J.-P., Driguez, H. & Haser, R. (1998). *EMBO J.* **17**, 5551–5562.
Pereira-Rodríguez, A., Fernández-Leiro, R., González-Siso, M. I., Cerdán, M. E., Becerra, M. & Sanz-Aparicio, J. (2012). *J. Struct. Biol.* **177**, 392–401.
Sakamoto, Y., Nakade, K. & Konno, N. (2011). *Appl. Environ. Microbiol.* **77**, 8350–8354.
Sambrook, J. & Russell, D. W. (2001). *Molecular Cloning: a Laboratory Manual.* New York: Cold Spring Harbor Laboratory Press.
Terwilliger, T. C. & Berendzen, J. (1999). *Acta Cryst.* D**55**, 1872–1877.
Tsai, L.-C., Hsiao, C.-H., Liu, W.-Y., Yin, L.-M. & Shyur, L.-F. (2011). *Biochem. Biophys. Res. Commun.* **407**, 593–598.
Umemoto, N., Kakitani, M., Iwamatsu, A., Yoshikawa, M., Yamaoka, N. & Ishida, I. (1997). *Proc. Natl Acad. Sci. USA*, **94**, 1029–1034.
Van Petegem, F., Collins, T., Meuwis, M. A., Gerday, C., Feller, G. & Van Beeumen, J. (2003). *J. Biol. Chem.* **278**, 7531–7539.
Vedadi, M. *et al.* (2006). *Proc. Natl Acad. Sci. USA*, **103**, 15835–15840.
Wallace, A. C., Laskowski, R. A. & Thornton, J. M. (1995). *Protein Eng.* **8**, 127–134.

Winn, M. D. *et al.* (2011). *Acta Cryst.* D**67**, 235–242.
Wojtkowiak, A., Witek, K., Hennig, J. & Jaskolski, M. (2012). *Acta Cryst.* D**68**, 713–723.
Wojtkowiak, A., Witek, K., Hennig, J. & Jaskolski, M. (2013). *Acta Cryst.* D**69**, 52–62.
Wu, H.-M., Liu, S.-W., Hsu, M.-T., Hung, C.-L., Lai, C.-C., Cheng, W.-C., Wang, H.-J., Li, Y.-K. & Wang, W.-C. (2009). *J. Biol. Chem.* **284**, 26708–26715.
Zechel, D. L. & Withers, S. G. (1999). *Acc. Chem. Res.* **33**, 11–18.
Zhang, R., Minh, T., Lezondra, L., Korolev, S., Moy, S. F., Collart, F. & Joachimiak, A. (2005). *Proteins*, **60**, 561–565.